Journal of Power Sources 246 (2014) 313–321

Contents lists available at ScienceDirect

Journal of Power Sources

journal homepage: www.elsevier.com/locate/jpowsour

A novel alcohol-thermal synthesis method of calcium zincates negative electrode materials for Ni–Zn secondary batteries

Ruijuan Wang [a], Zhanhong Yang [a,b,*], Bin Yang [a], Xinming Fan [a], Tingting Wang [a]

[a] College of Chemistry and Chemical Engineering, Central South University, Changsha 410083, China
[b] Key Laboratory of Resource Chemistry of Nonferrous Metals, Ministry of Education, Central South University, Changsha 410083, China

HIGHLIGHTS

- Calcium zincates were synthesized by alcohol-thermal method for the first time.
- The crystallization of as-prepared calcium zincate was well, and the particle size was small.
- The samples synthesized in the ethanol exhibited best electrochemical properties.

ARTICLE INFO

Article history:
Received 22 May 2013
Received in revised form
13 July 2013
Accepted 25 July 2013
Available online 2 August 2013

Keywords:
Calcium zincates
Alcohol-thermal method
Electrochemical property
Nickel–zinc secondary batteries

ABSTRACT

Calcium zincates are synthesized using ZnO and $Ca(OH)_2$ in different alcohol solutions by the alcohol-thermal method. Through the scanning electron microscopy (SEM), transmission electron microscope (TEM) and high resolution transmission electron microscope (HRTEM) analysis, the as-prepared samples with small particles are well-crystallized. Additionally, the morphologies of as-prepared calcium zincates are distinct in different reaction solvents such as ethanol, isopropanol and *n*-butanol, and the calcium zincates synthesized in the ethanol and isopropanol solutions have more excellent crystallinity. As the negative electrode materials for Ni–Zn batteries, the electrochemistry properties of calcium zincates are examined by cyclic voltammetry (CV), electrochemical impedance spectroscopy (EIS) and galvanostatic charge–discharge testing techniques. The results imply that calcium zincates synthesized in the ethanol solution have lower polarization and better reversibility. The cycle performance analysis shows the as-prepared calcium zincates have a very greatly improvement in cycle life and discharge capacity compared with other methods. All of the test results show that the calcium zincates synthesized in the ethanol solution exhibit the best electrochemical performances.

1. Introduction

The Zn electrodes in Ni–Zn secondary batteries have received considerable research attentions for their high specific energy density, low cost and environmental friendliness [1]. However, the development of Ni–Zn secondary batteries are still limited by the short life-cycle and poor electrochemical battery performance of zinc anodes, which mainly results from the dendritic growth, shape change and high solubility of the zinc discharge produce dendritic growth duct in concentrated alkaline KOH solution [2,3]. Hence, many attempts have been made to conquer the problems. Especially using additives in the electrodes or electrolytes, some of them are various inorganic species, namely, $Ca(OH)_2$ [4], $In(OH)_3$ [5], Bi_2O_3 [5,6] and $PbCl_2$ [7] were used in zinc electrodes to overcome the problems mentioned above. All of these inorganic additives, $Ca(OH)_2$ seems a promising candidate [8], because calcium zincates is formed in the charge-discharge process and it can inhibit the migration of zinc electrode active material.

Calcium zincates have been directly applied to the zinc electrode active materials by some researchers [9–11], and the results show calcium zincates are beneficial to zinc electrode active material and the electrochemical performances are superior to the physical mixture of $Ca(OH)_2$ and ZnO. Hence, synthetic methods of calcium zincates have been increasingly studied. Some researchers [12–17] have reported that the calcium zincates were synthesized by chemical co-precipitation. Other researchers [8,9] reported that the ball mill method was used to synthesize the calcium zincates.

Wang [18] has reported calcium zincates were synthesized by hydrothermal method. Hydrothermal method needs higher reaction temperatures, resulting in dehydration of the partial calcium zincates

* Corresponding author. College of Chemistry and Chemical Engineering, Central South University, Changsha 410083, China. Tel./fax: +86 0731 88879616.
E-mail addresses: zhyang@mail.csu.edu.cn, zhongnan320@gmail.com (Z. Yang).

0378-7753/$ – see front matter © 2013 Elsevier B.V. All rights reserved.
http://dx.doi.org/10.1016/j.jpowsour.2013.07.097

and formed irregular particles, which produce many defects. In this paper, calcium zincates were synthesized by alcohol-thermal method which based on hydrothermal method. The ethanol, isopropanol and *n*-butanol were used as the reaction medium instead of the water in this method.

2. Experimental

2.1. The synthesis of calcium zincates

The calcium zincates were prepared as following: $Ca(OH)_2$ (0.02 mol) and ZnO (0.0404 mol) were mixed and drilled into powder, then put them into the azeotrope (100 mL) which consists of alcohols and distilled water, then transferred the above reaction solution to a reaction kettle and continually stirred for 10 min, then sealed the kettle and kept it in thermostatic drying closet, reacting at azeotropic temperature for ten hours, filtering, washing and drying at 60 °C, then the product of calcium zincates powders were collected and packed in a PE bag for further examination and use.

2.2. The characterization of the calcium zincates samples

The morphology of the calcium zincates samples was characterized by scanning electron microscope (SEM, JSM-6360LV) and transmission electron microscope (TEM) and high resolution transmission electron microscope (HRTEM) (JEM-2100F, JEOL, Japan). Fast Fourier transformation (FFT) image analysis was accomplished by capturing constant magnification HRTEM and subsequently processing and analyzing these. The X-ray diffraction (XRD) was performed on a D500 (Siemens) diffractometer (36 kV, 30 mA) using Cu Kα radiation at a scanning rate of $2\theta = 8^\circ$ min^{-1}. The Fourier transform infrared (FTIR) spectroscopy was conducted on a Nicolet Nexus-670 FT-IR spectrometer (as KBr discs, with wave number 400–4000 cm^{-1}, resolution 0.09 cm^{-1}, and the weight of measured sample is 2 mg).

2.3. The preparation and electrochemical measurements of the calcium zincates electrodes

The calcium zincates electrodes were prepared by incorporation slurries [19] containing 80 wt.% calcium zincates, 5 wt.% Zn powder (95%, Traditional Chinese Medicines Chemical Reagent), 10 wt.% acetylene black and 5 wt.% additives of polytetrafluoroethylene (PTFE, 60 wt.%, in diluted emulsion). Copper mesh (1.0 cm × 1.0 cm in size) was served as the current collector and the calcium zincates electrodes were roll-pressed to a thickness of 0.2 mm. Then, the obtained calcium zincates electrodes were dried at 60 °C. The positive electrode was the commercial sintered $Ni(OH)_2$ electrode (Tianjin City Fine Chemical Research Institute) whose capacity was much larger than calcium zincates electrode for making full use of the active material in calcium zincates electrode. The electrolyte is solution of 6 M KOH saturated with ZnO. All the cells were pre-activated for 5–8 times by the following operations: The cells were charged at constant current of 0.1 C for 600 min, and discharged at constant current of 0.2 C to a cut-off voltage of 1.2 V.

The cyclic voltammetry (CV) tests of the calcium zincates electrodes were examined on Electrochemical Workstation CS-350 (Wuhan Corrtest Instruments Co.) at room temperature (25 ± 2 °C) in 6 M KOH solution. The electrochemical impedance spectroscopy (EIS) tests of the calcium zincates electrodes were examined on a PARSTAT 2273-type electrochemical system (Princeton Applied Research) in 6 M KOH solution at room temperature (25 ± 2 °C). The working electrode was pre-activated calcium zincates electrode mentioned above. A large area sintered $Ni(OH)_2$ electrode was severed as counter electrode and an Hg/HgO electrode was used as reference electrode. The cyclic voltammetry was carried out at a scanning rate of 1 mV s^{-1} over a shifting range from −1.05 V to −1.65 V. The applied frequency range for electrochemical impedance spectroscopy was between 0.01 Hz and 100 KHz, and the amplitude of AC signal was set at 10 mV.

The batteries were galvanostatically charged and discharged in a battery test system (Neware BST-5v/10 mA) with a current density of 1 C for a cut-off voltage of 1.2 V at room temperature (25 ± 2 °C). The cycling tests were performed in a battery test system (Neware BST-5v/20 mA) at room temperature, and the batteries were charged at 2 C rate for 0.5 h and discharged at 2 C rate down to 1.2 V cutoff voltage.

In all the above experiments, all of the reagents were AR grade and the electrolyte was prepared with deionized water.

3. Results and discussion

3.1. The surface morphology of the calcium zincates samples

Alcohol-thermal method has low temperature, short reaction time and simple washing process. Compared with the hydrothermal method, its lower temperature will not lead to dehydrated product, resulting in the synthetic calcium zincates particles regular and small. The SEM images of the calcium zincates (CaZn) prepared in different alcohols solutions are shown in Fig. 1. The *eth*-calcium zincates (*eth*-CaZn) were synthesized by alcohol-thermal method in the ethanol and distilled water azeotrope mentioned above. Similarly, *iso*-calcium zincates (*iso*-CaZn) and *but*-calcium zincates (*but*-CaZn) were prepared in the isopropanol or *n*-butanol solutions instead of ethanol, respectively. The SEM images of *eth*-calcium zincates sample (sample A) are shown in Fig. 1A, B and C shows the SEM images of *iso*-calcium zincates sample (sample B) and *but*-calcium zincates sample (sample C), respectively. The sample A is hexagonal prism material as shown in Fig. 1A. From Fig. 1c and d, it could be clearly observed that sample B is lamellar material. Fig. 1c and f shows that the crystallized of sample C has two structures of hexagonal prism and lamellar. It could be seen that the particle sizes of the three kinds of calcium zincates are about 200–300 nm.

For confirming the results mentioned above, TEM, HRTEM and FFT characterization are used as shown in Fig. 2. Firstly, the TEM images of *eth*-calcium zincates, *iso*-calcium zincates and *but*-calcium zincates (Fig. 2a, c and e) show the different morphology and size (hexagonal prism for *eth*-calcium zincates, lamellar for *iso*-calcium zincates and two structures of hexagonal prism and lamellar for *but*-calcium zincates), which also have been shown by SEM images. Secondly, for *eth*-calcium zincates, the clearly lattice fringes with lattice spacing of 0.329 and 0.74 nm are corresponding to those of the (200) and (100) facets, respectively (Fig. 2b). Fig. 2d displays the HRTEM images of *iso*-calcium zincates, which show clearly two lattice fringes with a lattice spacing of 0.341 and 0.683 nm, corresponding to that of the (200) and (100) facets, respectively. Likewise, the relatively unclear lattice fringes of *but*-calcium zincates with lattice spacing of 0.378 and 0.628 nm are corresponding to those of the (200) and (100) facets, respectively (Fig. 2f). Meanwhile, it can be observed that the *eth*-calcium zincates and *iso*-calcium zincates have the well crystalline nature. Thirdly, the corresponding FFT (insert in the right-upper part of Fig. 2b, d and e) indicated that the calcium zincates are a single crystal in nature. Based on the above analysis, it can be concluded that the three kinds of as-prepared materials are calcium zincates with different morphology and crystallinity. In this work, the calcium zincates with high crystalline were synthesized in the ethanol and isopropanol solvent.

The three types of calcium zincates in different alcohol solvents have different morphologies and crystallinity. The main reason is that the different azeotropes have different azeotropic temperature and at

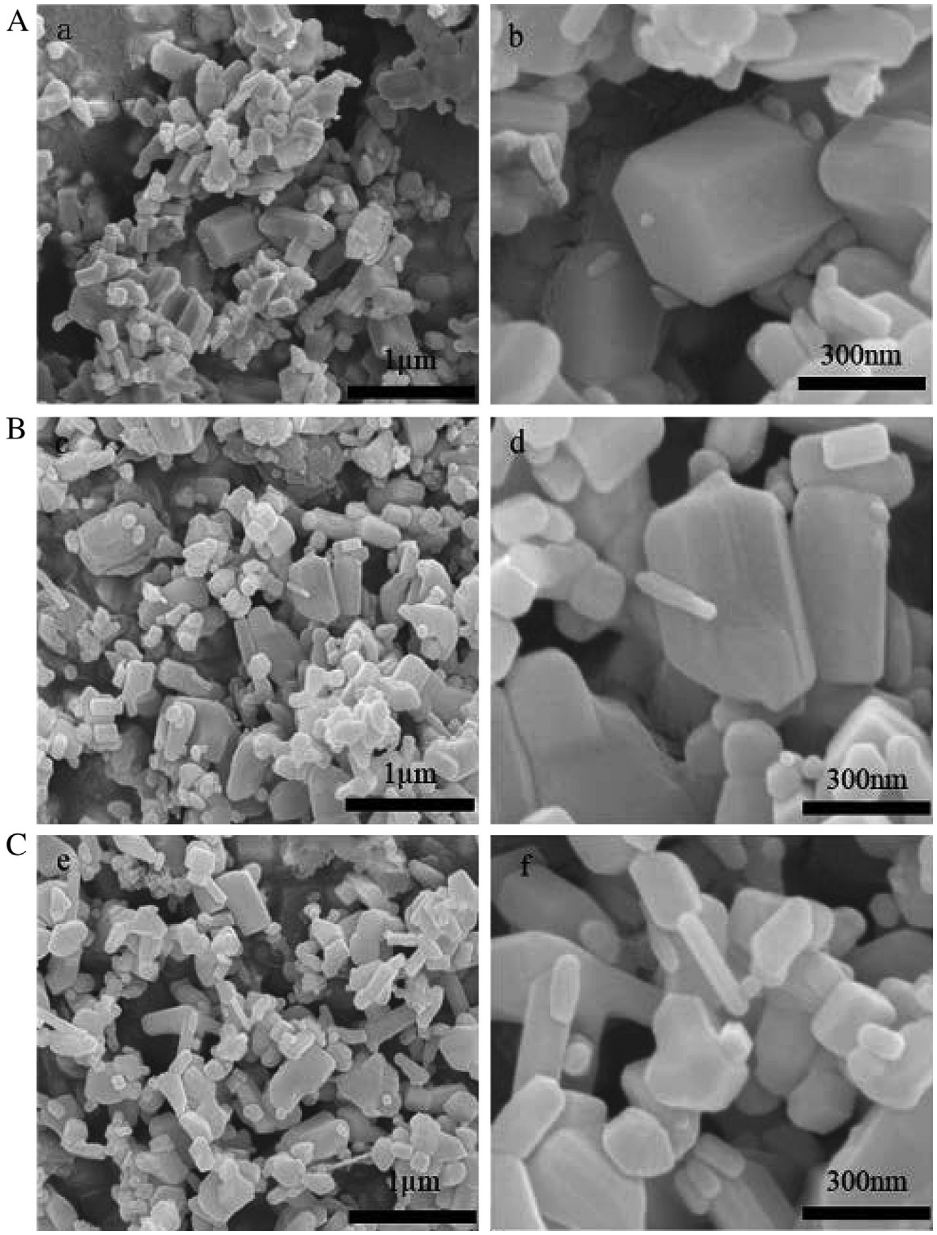

Fig. 1. The typical SEM micrograph of calcium zincates samples: (A) *eth*-calcium zincates for (a) 60 000 times magnification and (b) 200 000 times magnification; (B) *iso*-calcium zincates for (c) 60 000 times magnification and (d) 200 000 times magnification; (C) *but*-calcium zincates for (e) 60 000 times magnification and (f) 200 000 times magnification.

different temperature the crystal nucleation have different rates of generation and growth. If the generation speed of the nucleation is fast and growth speed is slow, it would generate more nucleation number, crystal structure is perfect. Different types of azeotropes have different azeotropic temperature, such as azeotropic temperature for the azeotropic mixture of ethanol and water is 90 °C, azeotropic temperature for the azeotropic mixture of isopropanol and water is 92 °C, and that for the azeotropic mixture of *n*-butanol and water is 105 °C. Temperature affects solute mass transfer coefficient, the generation speed of the nucleation is affected correspondingly, so that the size and morphology of the crystal particles are affected. Because of the small difference among the three kinds of azeotropic temperatures, there is little difference in particle size. The morphology of calcium zincates synthesized by hydrothermal method [18] was irregular, and the particle sizes were about 5 μm. Calcium zincates synthesized by solid-phase [20] were well crystallized tetragonal, and the particle sizes were about 45 μm. For the alcohol-thermal method, the synthesized samples have more regular of morphology structure and a smaller particle size.

3.2. The XRD analysis of calcium zincates samples

The XRD patterns of the calcium zincates prepared in three different kinds of alcohols are shown in Fig. 3. The three kinds of calcium zincates show the characteristic peaks at $2\theta = 14.10^\circ$ and 28.48°, which corresponds to the reflections of (100) and (200) in the XRD standard spectrum of calcium zincates, indicating that the calcium zincates can be successfully prepared by alcohol-thermal method. From Fig. 3, it can be seen that the weak peaks at $2\theta = 31.85$, 34.35 and 36.23, suggesting that it exists ZnO impurity in the samples. Based on the XRD spectrum, it could be concluded that the main crystal in the sample was calcium zincates. There were some weak peaks of ZnO and no peak of $Ca(OH)_2$, suggesting that the conversion efficiency of reactants is high, the excessive ZnO

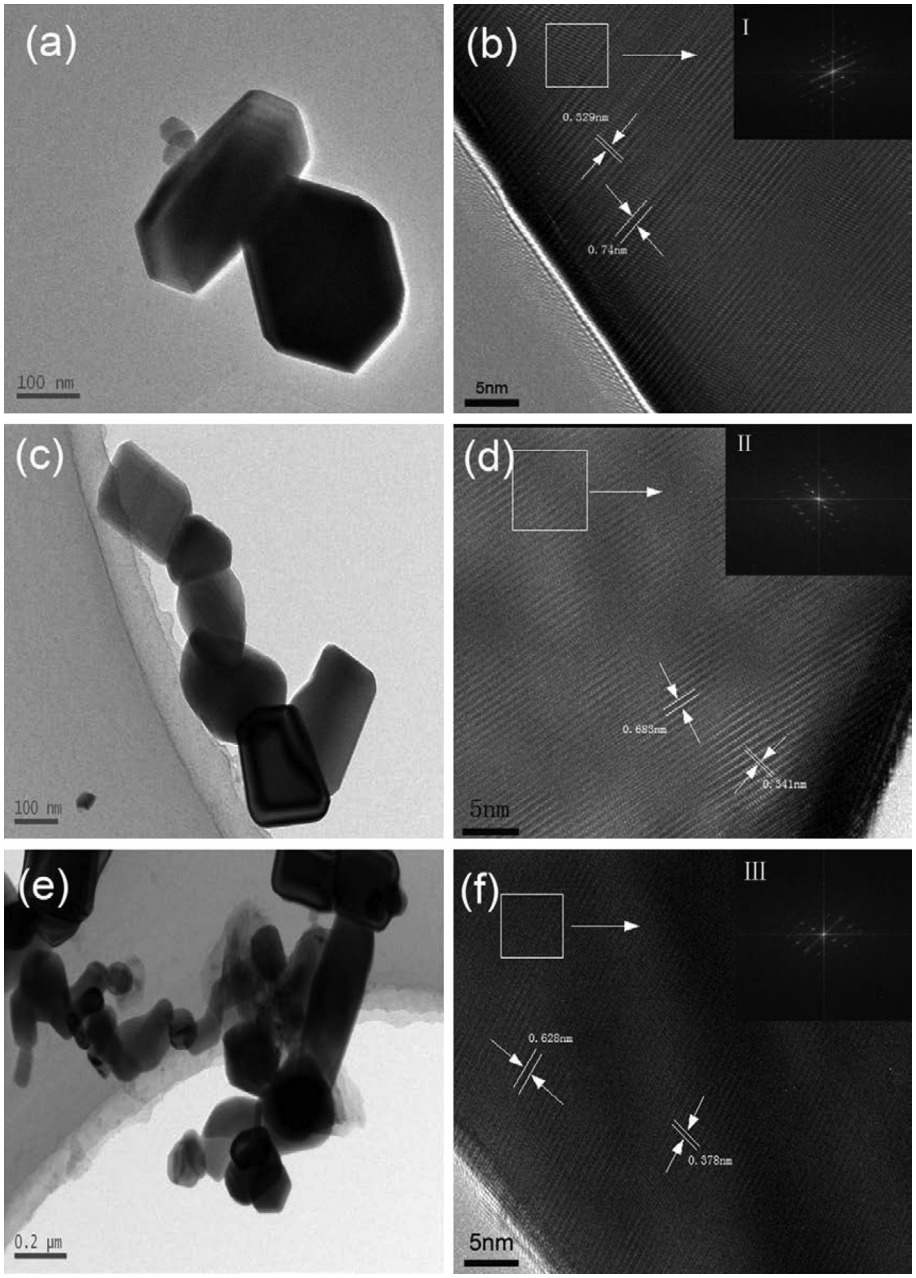

Fig. 2. TEM, HRTEM and FFT images of calcium zincates, (a, b) *eth*-calcium zincates; (c, d) *iso*-calcium zincates; (e, f) *but*-calcium zincates.

could enable $Ca(OH)_2$ convert into calcium zincates completely. In addition to that, the excessive ZnO could work as the active material of the electrodes, which would not affect the electrochemical properties of the calcium zincates electrodes. For the diffraction peaks of calcium zincates, the samples prepared in ethanol solution are relatively sharp and narrow, indicating that the sample is well-crystallized.

3.3. The FT-IR analysis of calcium zincates samples

Fig. 4 shows that all three kinds of samples appear obvious absorption peaks at about 3640 cm^{-1}, 3450 cm^{-1}, 1445 cm^{-1}, 1083 cm^{-1}, 773 cm^{-1}, 459 cm^{-1}. The broad band at 3640 cm^{-1} can be ascribed to the stretching of OH^- groups, but the broad bands at 3450 cm^{-1}, 1445 cm^{-1} are related to the absorption of crystal water. The sample synthesized in *n*-butanol solution has weak peak near 3450 cm^{-1}, indicating that the sample has less crystal water. The bands at 1083 cm^{-1} and 773 cm^{-1} are indicated to Ca—O stretching vibrations. The band at 459 cm^{-1} can be assigned to Zn—O stretching vibrations. All of the above is showing that the samples are calcium zincates, and they are very similar to the infrared spectrum of calcium zincates prepared by hydrothermal and co-precipitation methods [18].

3.4. The cyclic voltammetry results of the calcium zincates electrodes

The CV measurements were carried out to study the electrochemical performance of calcium zincates prepared by alcohol-thermal method, and the recorded CV curves are given in Fig. 5. As shown in Fig. 5, the potential sweep starts from −1.05 V, going toward the cathodic direction, and reversed to the anodic direction

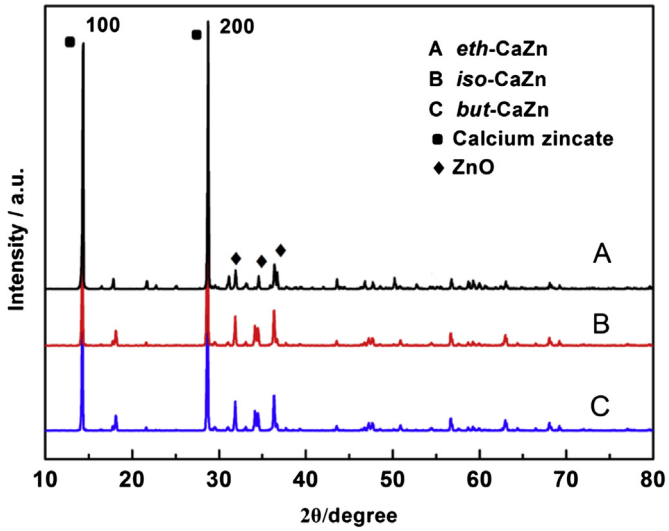

Fig. 3. XRD pattern of as-prepared calcium zincates samples: (A) *eth*-calcium zincates; (B) *iso*-calcium zincates; (C) *but*-calcium zincates.

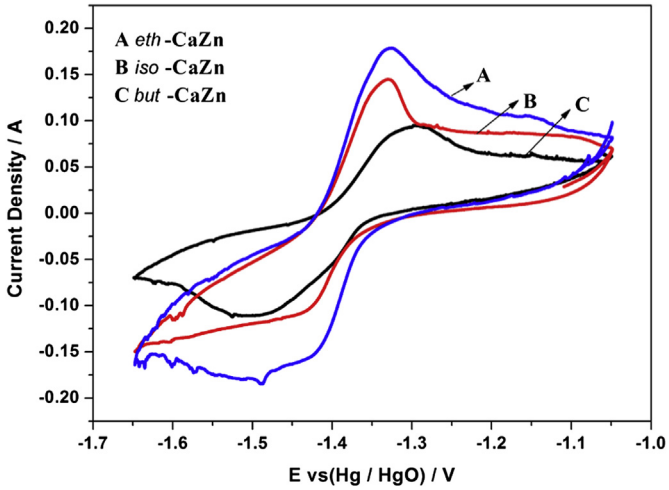

Fig. 5. The cyclic voltammograms of the electrodes with as-prepared calcium zincates samples: (A) *eth*-calcium zincates; (B) *iso*-calcium zincates; (C) *but*-calcium zincates.

at −1.65 V. The calcium zincates electrodes, which were synthesized in the azeotropic mixture of ethanol and water, azeotropic mixture of isopropanol and water, azeotropic mixture and *n*-butanol and water, are labeled as electrodes A, electrodes B and electrodes C respectively. For the cathodic sweep, it can be seen that the peaks of electrodes A and B begin to appear at −1.42 V and electrodes C appear at −1.48 V. The cathodic current density was higher at the lower potential region, indicating there were two kinds of reduction reaction. The one is reduction reaction of calcium zincates and it can be described as Eq. (1).

$$Ca(OH)_2\cdot 2Zn(OH)_2\cdot xH_2O + 4e \rightarrow Ca(OH)_2 + 2Zn + xH_2O + 4OH^- \quad (1)$$

The other is conversion of calcium zincates which is ascribed to the dissolution of calcium zincates in alkaline electrolyte, the conversion reaction occurred on the surface of calcium zincates can be represented as following:

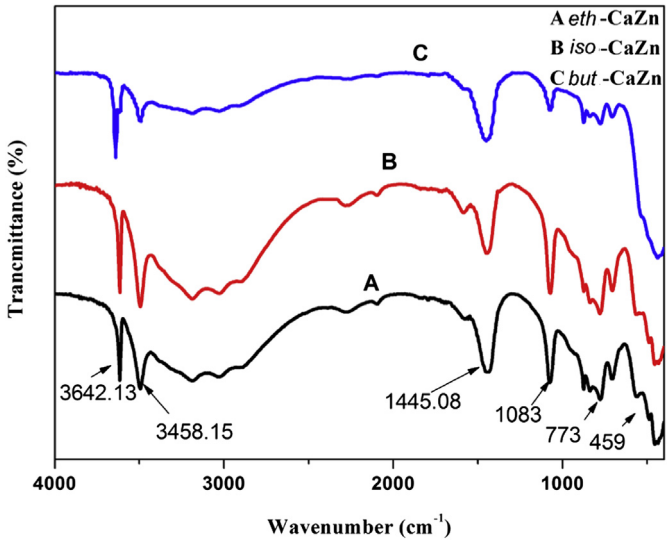

Fig. 4. FT-IR spectra of as-prepared calcium zincates samples: (A) *eth*-calcium zincates; (B) *iso*-calcium zincates; (C) *but*-calcium zincates.

$$Ca(OH)_2\cdot 2Zn(OH)_2\cdot xH_2O + 4OH^- \rightarrow 2Zn(OH)_4^{2-} + Ca(OH)_2 + xH_2O \quad (2)$$

The surface conversion products $Zn(OH)_4^{2-}$ can be reduced into Zn, the reduction reaction can be represented as Eq. (3):

$$Zn(OH)_4^{2-} + 2e \rightarrow Zn + 4OH^- + H_2O \quad (3)$$

As the accumulation of surface conversion products and reduction of $Zn(OH)_4^{2-}$, there are two kinds of reduction reaction (Eq. (1) and Eq. (3)) occurred at the lower potential region and the current density increase.

For electrodes C, the anodic peak of reduction reaction of conversion products on the surface appear at −1.48 V, which was shifted in the more positive direction in comparison with that electrodes B. The more positive shift is ascribed to the higher concentrations of $Zn(OH)_4^{2-}$. The electrode reaction is as Eq. (3) and the well-known Nernst equation are as follows:

$$\Phi = \varphi^{\theta} + (0.0592/2)\lg\left(\left[Zn(OH)_4^{2-}/[OH^-]^4\right]\right) \quad (4)$$

Due to the different morphologies and microstructures of the three kinds of calcium zincates, the solubility and the rate of conversion reaction on the surface were different. Just as discussed before, sample C has irregular morphology, the irregular morphology structure will lead to the higher solubility of the sample in alkaline electrolyte. So the concentration of $Zn(OH)_4^{2-}$ in alkaline electrolyte is higher, which make the reaction of Eq. (3) potential shift positively. Therefore, the two kinds of reaction occurred simultaneously at −1.48 V. However, sample A and B had regular morphology and the lower solubility in alkaline electrolyte, the rate of conversion reaction on the surface was relatively slow. Compared with samples B, samples A with hexagonal prism had smaller solubility, the conversion reaction on surface will be stopped when the *eth*-calcium zincates are consumed, so the reduction Eq. (3) will be ended when the $Zn(OH)_4^{2-}$ was reduced completely and it achieved the maximum values of current at −1.48 V. For electrode B, because of the relatively higher solubility than sample A, the reduction reaction of conversion products on the surface had always been occurred. The sufficient $Zn(OH)_4^{2-}$ can continuously supply to reduction reaction of Eq. (3), then the

current density was increased as the two kinds of reduction reactions occurred.

It is well known that a more negative potential for cathodic peaks means a larger polarization [21]. Compared with electrode C, the potentials of electrodes A and B were positively shifted by 60 mV, which indicated that electrodes A and B had a lower polarization process. There are two reasons for the electrode polarization, one is electrochemical polarization, which comes from the slow electron transfer, and the other is concentration polarization, which derives from slow mass transfer. The three kinds of electrodes were prepared and tested in the same conditions, so the different electrode polarization of the three kinds of electrodes is due to the different electron transfer. A good crystallization help to electron transfer, so the lower polarization comes from the good crystallization of active materials.

During the anodic process, a clear distinction can be seen that there is only one anodic peak located at −1.32 V for electrode B, but there are two anodic peaks for electrode A, which appeared at −1.32 V and −1.14 V. This two anodic peaks phenomenon is an important characteristic for anodic dissolution of zinc and has been deeply studied by previous works [22–24]. The two anodic peaks of electrode A correspond to two processes of anodic dissolution. There is no doubt that the reaction at the equilibrium potential gives birth to the zincates ion, $Zn(OH)_4^{2-}$, by a probable three-step process represented by the overall reaction [23,24] and Eq. (5) must be the one occurring in the first peak of −1.32 V.

$$Zn + 4OH^- \rightarrow Zn(OH)_4^{2-} + 2e \quad (5)$$

The peak at −1.14 V occurs when the reaction (5) has proceeding for some time at a lower potential and consequently when there has been an inadequate contact between active materials and OH^- ion from the reaction layer [22]. The two anodic peaks caused by the inadequate contact were reported [23,24]. A probable reaction corresponding to this peak of −1.14 V is Eq. (6).

$$Zn + 3OH^- \rightarrow Zn(OH)_3^- + 2e \quad (6)$$

Compared to electrodes A and B, the anodic peak of electrode C moves towards positive direction and is located at −1.29 V, which indicates that electrode C have a larger polarization. The reason of the anodic polarization is similar to cathodic polarization, and that resulted from the bad crystallization of the electrode C. Moreover, the current density is larger, indicating that it is much easier for the occurrence of oxidation–reduction reaction compared with ball-milled [9,10] method and solid-phase [20] method. Meanwhile, *eth*-calcium zincates and *iso*-calcium zincates show higher anodic peak current and larger anodic peak area. The anodic process reflects the discharge process of calcium zincates. The increase in anodic peak area and anodic peak current means that *eth*-calcium zincates and *iso*-calcium zincates possess the higher electrochemical activity, and can deliver more discharge-capacity than *but*-calcium zincates. The potential interval between an anodic peak and a cathodic peak is taken as a measurement of the reversibility of electrode reaction, and the smaller the interval, the better the reversibility. The potential interval of electrode A is the smallest, which means the electrode A has the highest reversibility of the electrode reaction. In order to further illustrate the reversibility of the electrode A, the relation graph of anodic peak current against square root of scan rate is shown in Fig. 6. It can be seen that there is a good linearity relationship between anodic peak currents and the different scan rate. There is slightly partial at the high scan rate, which may results from the surface kinetic factors between active material, conductive agent and electrolyte. In general, this electrode system is mainly controlled by diffusion, and the

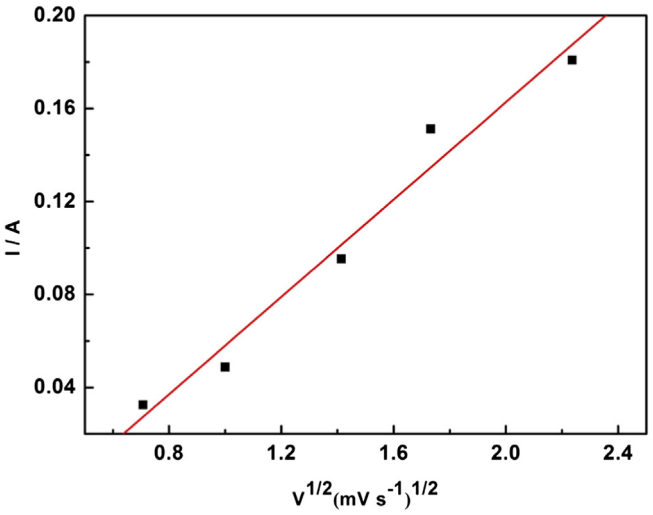

Fig. 6. The dependence of anodic peak current against square root of scan rate in the zinc electrodes with calcium zincates samples synthesized in the ethanol solution.

electrochemical reaction of the electrode in this environment is a quasi-reversible process.

Consequently, in the above discussion, electrodes A and B have a lower polarization process and electrode A has the highest reversibility of the electrode reaction. That is to say that *eth*-calcium zincates and *iso*-calcium zincates possess the better electrochemical activity and *eth*-calcium zincates exhibit the best performance.

3.5. The electrochemical impedance spectroscopy of the calcium zincates electrodes

Fig. 7a presents the impedance diagrams for the calcium zincates electrodes. All Nyquist plots included a high-frequency capacitive semicircular loop and a low-frequency straight line. The high-frequency capacitive semicircular loop can be ascribed to the charge-transfer resistance (R_{ct}) in parallel with the double-layer capacitance, and the slope in the low-frequency region is most probably caused by the diffusion of OH^- in the calcium zincates electrodes [25]. The equivalent circuit used to fit the EIS spectra is reported in Fig. 7b, where CPE represents the constant phase element for a porous electrode, *Re* designates the total ohmic resistance, which includes the resistance of the electrolyte, current collector, electrode materials. etc., R_{ct} is the charge-transfer resistance. The radius of capacitive loop can reflect the values of charge-transfer resistance for the calcium zincates electrodes.

The element parameters (Table 1) can be calculated by the ZSimpWin software. According to the equivalent circuit, the fitted R_{ct} of *eth*-calcium zincates electrode, *iso*-calcium zincates electrode and *but*-calcium zincates electrode were 2.62 Ω cm^2, 2.85 Ω cm^2 and 2.87 Ω cm^2, respectively. A large R_{ct} means that the electrochemical reaction is more difficult and leads to an increase in the electrochemical polarization. The most possible reason is that the crystallinity of calcium zincates prepared in the ethanol and isopropanol solutions are better than in the *n*-butanol solution, a well crystallization may be beneficial to electron transfer. From Fig. 1, we can see that the *eth*-calcium zincates have a regular hexagonal prism structure and the *iso*-calcium zincates have a regular lamellar structure, and the *but*-calcium zincates have structures both of hexagonal prism and lamellar. The regular structure may reduce the charge-transfer resistance and contribute to charge-transfer. The regular hexagonal prism of the *eth*-calcium zincates and the regular lamellar of the *iso*-calcium zincates increases the direct contact between the active materials and the electrolyte, enhances

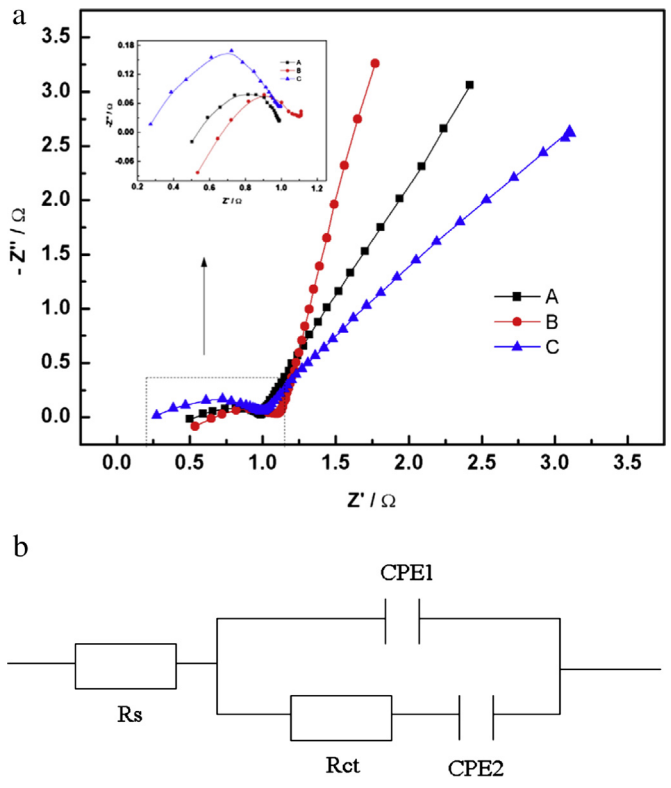

Fig. 7. (a). The electrochemical impedance spectra of the electrodes with as-prepared calcium zincates samples: (A) *eth*-calcium zincates; (B) *iso*-calcium zincates; (C) *but*-calcium zincates. (b). The equivalent circuit model for the EIS spectra.

the charge transfer between the core calcium zincates and the electrolyte. The main reason is attributed to the regular hexagonal prism and lamellar calcium zincates have regular and smaller particles, leading to increase the passageways for OH^- and the specific surface area of active material. The charge-transfer resistance is inversely proportional to the current density, and the formula is as following:

$$\frac{1}{R_{ct}} = \left(\frac{\partial I_F}{\partial E}\right)_{ss} \quad (7)$$

I_F – Faraday current density

E – Electrode potential

From Fig. 7a and Table 1, it can also found that the *eth*-calcium zincates electrode showed the smallest ohmic resistance (R_s), suggesting that *eth*-calcium zincates particles can produce a good electrical contact between active core material and copper mesh, which may help to counteract the negative influence of the larger charge-discharge resistance to the electrochemical reaction rate [19].

Table 1
The values of charge transfer resistance, capacitance parameters and Warburg resistance derived from the ZSimpWin software.

Anode type	R_{ct} (Ω cm^2)	CPE2 (Ω^{-1} cm^{-2})	R_s (Ω cm^2)
eth-CaZn	2.62	0.02562	0.9839
iso-CaZn	2.85	0.03427	1.110
but-CaZn	2.87	0.03943	1.003

From the results of EIS, it can be found that calcium zincates prepared in the ethanol has the lowest resistance. The smaller the resistance, the larger peak of current density in the CV tests, so the two results are consistent from Figs. 5 and 7a.

3.6. The properties of galvanostatic charge and discharge

Fig. 8 displays the typical galvanostatic charge–discharge curves of the test cells with calcium zincates electrodes at the 20th cycle. From Fig. 8a, it can be seen that the maximum charge voltage of the three samples are different, battery A reached the charge voltage plateau quickly and then remains almost constant, which indicates battery A has the best electrochemical property. The stable voltage can be ascribed to the fact that battery A has the smaller battery internal resistance and lower polarization, which is also proved by CV results.

Meanwhile, as observed from charge–discharge curves of Fig. 8a and b, the battery of *eth*-calcium zincates presents a lower charge

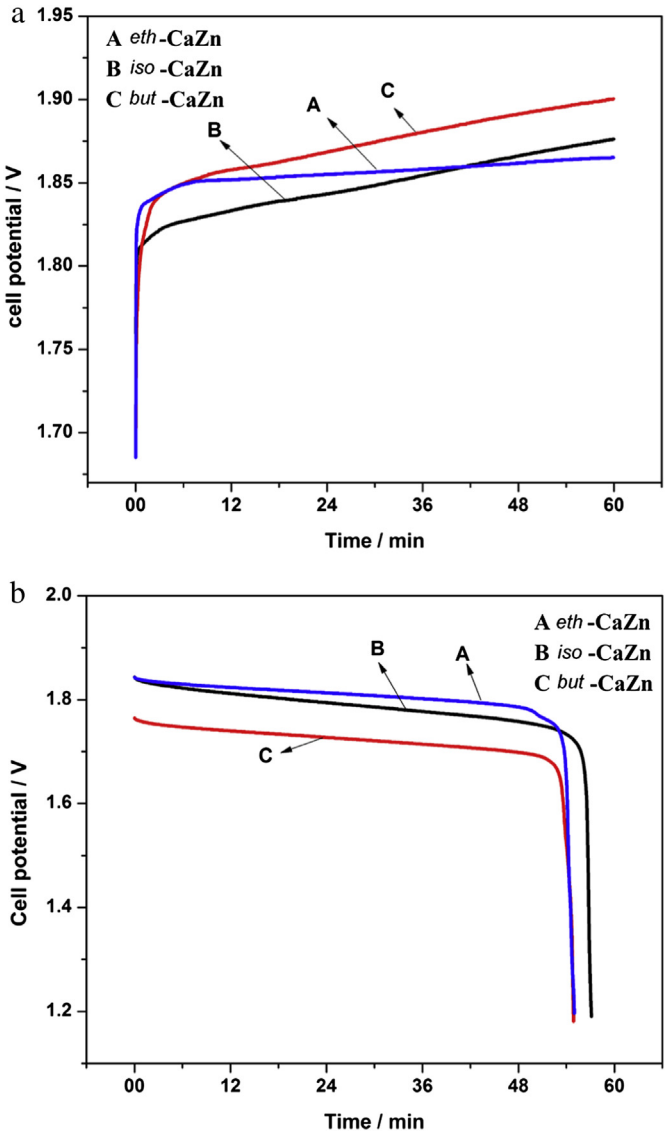

Fig. 8. (a). The typical galvanostatic charge curves of Ni–Zn secondary batteries with as-prepared calcium zincates samples: (A) *eth*-calcium zincates; (B) *iso*-calcium zincates (C) *but*-calcium zincates. (b). The typical galvanostatic discharge curves of Ni–Zn secondary batteries with as-prepared calcium zincates samples: (A) *eth*-calcium zincates; (B) *iso*-calcium zincates; (C) *but*-calcium zincates.

plateau voltage and higher discharge plateau voltage than that of *iso*-calcium zincates and *but*-calcium zincates. For *eth*-calcium zincates, the low charge plateau voltage conduces to the suppression of H_2 formation and the increase efficiency, and the high discharge plateau means high output energy and power. Just as discussed before, the samples A and B with good crystallization exhibit lower internal resistance, which results in a lower charge voltage and higher discharge voltage for good crystallization and regular structure materials. Due to the polarization in the cell reaction process, the battery voltage increases when charge, and reduces when discharge. The voltage decrease or increase is mainly ascribed to internal resistance and electrode polarization of the battery. In our experimental, all the test factors except electrode materials are the same. So the difference caused by the internal resistance is small and can be ignored. The voltage decrease or increase is mainly ascribed to the electrode polarization. The size of polarization can be obtained by the charge voltage and discharge voltage difference. As the above mentioned, battery A has the lower charge voltage and higher discharge voltage, indicating battery A has the smaller polarization.

From Fig. 8b, it can be also found that battery A has two discharge plateau voltage, the first plateau is near 1.8 V and discharge time lasts 50 min. But the second plateau is near 1.76 V and lasts 3 min. The two discharge plateau voltages are corresponding to the two anodic peaks in the CV figure. The discharge efficiencies of battery A, B and C are 92.6%, 95.3% and 93.5% respectively, it can be seen that all the three kinds of batteries have a good charge discharge property. Although the morphology and crystallization affect the internal resistance of calcium zincates electrodes, it should be noted that this phenomenon has no undesirable influence on the discharge capacity of Ni–Zn battery. It can be obtained by the calculation that the discharge capacity is about 341.2 mA h g^{-1} and the theoretical capacity of calcium zincate is 347 mA h g^{-1}. Meanwhile, the 5% conductive Zn-additive metal also takes part in the reaction, which increases the discharge capacity. Compared to sold-phase method [20], which electrodes not add zinc and practical capacity of calcium zincates is 195.8 mA h g^{-1}, the practical capacity of calcium zincates prepared by alcohol-thermal method is larger. The galvanostatic charge–discharge results imply that the three kinds of as-prepared calcium zincates all have a high discharge capacity and calcium zincates synthesized in the ethanol solution have the best electrochemical property.

3.7. The cycle performance analysis of calcium zincates electrodes

The cycling performances at the current density of 2C rate are presented in Fig. 9. As observed, all the electrodes suffer from low capacity for the first several cycles due to the incomplete activation of the active materials in the electrodes. During the subsequent cycles, the active material is gradually activated. As shown in Fig. 9, *eth*-calcium zincates electrode and *iso*-calcium zincates electrode not only deliver higher discharge capacity than *but*-calcium zincates electrode, but also show more cycle stability. These values indicate a good cycling stability that is much better than that of *but*-calcium zincates electrode. For the *eth*-calcium zincates electrode, as the cycling continued from 4th cycle up to the 200th cycle, a significant increase in the discharge capacity is observed from 318.5 mA h g^{-1} to 341.2 mA h g^{-1}. For comparison, *iso*-calcium zincates electrode shows relatively stable cycling performance, but its discharge capacity is lower than *eth*-calcium zincates electrode. However, *but*-calcium zincates electrode have the worst cycle performances, such as low discharge capacity and instable cycling performance. The relatively bad cycle performance is contributed to the irregular surface morphology and bad crystallization. Therefore, *eth*-calcium zincates and *iso*-calcium zincates exhibit both a larger discharge capacity and a better cycling stability compared with *but*-calcium zincates electrode. Nevertheless, compared to other methods [9,10,20], the cycle life and discharge capacity of the as-prepared calcium zincates are greatly improved.

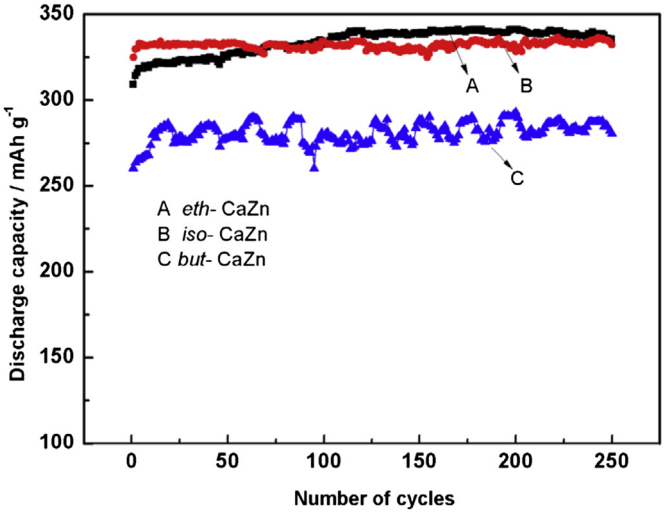

Fig. 9. Electrochemical cycle behavior of Ni–Zn batteries with as-prepared calcium zincates: (A) *eth*-calcium zincates; (B) *iso*-calcium zincates; (C) *but*-calcium zincates.

4. Conclusions

The XRD and FT-IR results show that calcium zincates can be successfully synthesized by alcohol-thermal method. Calcium zincates synthesized in the three kinds of solutions have different morphologies and crystallization. All the samples have well crystallization and small particle size, but *eth*-calcium zincates and *iso*-calcium zincates have more excellent crystallization. As the electrode materials of Ni–Zn battery, the as-prepared calcium zincates possessed high electrochemical activity, showed the excellent discharge capacity and cycle stability. Among the three kinds of calcium zincates, the *eth*-calcium zincates are best suitable for the negative electrode materials of Ni–Zn secondary batteries.

Acknowledgments

This work is supported by National Natural Science Foundation of China (No. 91023031) and Changsha Science and Technology Project of China in 2012 (No. K1203014-11) and Production, Teaching and Research Integrated Project of Guangdong Province and Ministry of Education (No. 2010B090400341).

References

[1] D. Coates, E. Ferreira, A. Charkey, J. Power Sources 65 (1997) 109–115.
[2] V. Ravindran, V.S. Muralidharan, J. Power Sources 55 (1995) 237–241.
[3] E.G. Gagnon, J. Electrochem. Soc. 133 (1986) 1989–1995.
[4] Y. Zheng, J.M. Wang, H. Chen, J.Q. Zhang, C.N. Cao, Mater. Chem. Phys. 84 (2004) 99–106.
[5] M. Yano, S. Fujitani, K. Nishio, Y. Akai, M. Kurimura, J. Power Sources 74 (1998) 129–134.
[6] J. McBreen, E. Gannon, J. Power Sources 15 (1985) 169–177.
[7] J.Q. Kan, H.G. Xue, S.L. Mu, J. Power Sources 74 (1998) 113–116.
[8] R.A. Sharma, J. Electrochem. Soc. 133 (1986) 2215–2219.
[9] X.M. Zhu, H.X. Yang, X.P. Ai, J.X. Yu, Y.L. Cao, J. Appl. Electrochem. 33 (2003) 607–612.
[10] H.B. Yang, H.C. Zhang, X.D. Wang, J.H. Wang, X.L. Meng, Z.X. Zhou, J. Electrochem. Soc. 151 (2004) A2126–A2131.
[11] J.X. Yu, H.X. Yang, X.P. Ai, X.M. Zhu, J. Power Sources 103 (2001) 93–97.
[12] C. Zhang, J.M. Wang, L. Zhang, C.N. Cao, J. Appl. Electrochem. 31 (2001) 1049–1054.
[13] Y.M. Wang, G. Wainwright, J. Electrochem. Soc. 133 (1986) 1869–1872.
[14] Y.M. Wang, J. Electrochem. Soc. 137 (1990) 2800–2803.

[15] R. Jain, T.C. Adler, F.R. McLarnon, E.J. Cairns, J. Appl. Electrochem. 22 (1992) 1039–1048.
[16] F. Ziegler, C.A. Johnson, Cem. Concrete Res. 31 (2001) 1327–1332.
[17] A. Pigaga, A. Selskis, M.G. Klimantaviciute, A. Sveikauskaite, Russ. J. Appl. Chem. 76 (2003) 80–84.
[18] S.W. Wang, Z.H. Yang, S.S. Shen, Q.W. Liang, L.H. Zeng, D.R. Liu, J. Chem. Res. 20 (2009) 64–73.
[19] S.W. Wang, Z.H. Yang, L.H. Zeng, J. Electrochem. Soc. 156 (1) (2009) A18–A21.
[20] S.W. Wang, Z.H. Yang, L.H. Zeng, Mater. Chem. Phys. 112 (1) (2008) 603–606.
[21] X. Fan, Z. Yang, R. Wen, B. Yang, W. Long, J. Power Sources 224 (2013) 80–85.
[22] Y.F. Yuan, J.P. Tu, H.M. Wu, C.Q. Zhang, S.F. Wang, X.B. Zhao, J. Power Sources 165 (2007) 905–910.
[23] J.P.G. Farr, N.A. Hampson, J. Electroanal. Chem. 13 (1967) 433–441.
[24] R.W. Powers, M.W. Breiter, J. Electrochem. Soc. 116 (1969) 719–729.
[25] D.Q. Zeng, Z.H. Yang, S.W. Wang, X. Ni, D.J. Ai, Q.Q. Zhang, Electrochim. Acta 56 (2011) 4075–4080.